Scaling of the nonlinear response of the surface plasmon polariton at a metal/dielectric interface

Alexandre Baron[1], Stéphane Larouche[1], Daniel J. Gauthier[2] and David R. Smith[1]

[1]Center for Metamaterials and Integrated Plasmonics, Department of Electrical and Computer Engineering, Duke University, Durham, North Carolina 27708, USA

[2]Department of Physics, Duke University, Durham, North Carolina 27708, USA

Abstract

Plasmonic systems involve interfaces containing both a metal and a dielectric material. In an effort to investigate the scaling of the nonlinear response of the surface plasmon polariton at a metal/dielectric interface, where both the metal and the dielectric present optical nonlinearity, we introduce a figure-of-merit that quantifies the contribution of the metal and the dielectric to the nonlinear response in this specific situation. In the case of self-action of the surface plasmon polariton for the gold/dielectric interface, we predict that the dielectric nonlinear response is dominant for strongly nonlinear dielectrics such as polydiacetylenes, chalcogenide glasses or even semiconductors. The gold nonlinear response is dominant only in cases involving weakly nonlinear dielectrics such as silicon dioxide or aluminium oxide. We verify the relevance of the metric by investigating the process of optical switching via the third-order nonlinear response and discuss which gold/dielectric combinations have better switching behaviors.

Nonlinear optics has enabled a variety of applications, including ultrafast lasers and amplifiers [1], optical frequency conversion [2] and nonlinear microscopy [3]. Another potential application that has garnered considerable interest in the past decades is all-optical switching [4]. Driven by the goal of making efficient nonlinear devices with low control powers or high sensitivities, efforts have focused on studying nonlinear optics at the nanoscale, notably in plasmonic systems.

Surface plasmon polaritons (SPPs) are oscillations of charge density waves coupled to photons at a metal-dielectric interface [5]. SPPs stand out compared to other optical modes because their confinement is not restricted by the diffraction limit. As a result, SPPs concentrate fields at subwavelength scales to enhance the nonlinear response in metallic nanoparticles as well as on extended metal surfaces [6-8]. For almost two decades now, many theoretical proposals and experimental realizations have studied the nonlinear response of plasmonic systems, giving rise to the field of nonlinear plasmonics. Furthermore, the field of nonlinear

metamaterials, in which artificial materials can be designed and fabricated that enhance nonlinear phenomena at optical frequencies, overlaps with nonlinear plasmonics [9].

Studies of nonlinear plasmonic systems or metamaterials include nonlinear plasmonic waveguides [10-15], nonlinear self-action [16], active control [17], nanofocusing [18], nonlinear switching [19,20] and four-wave mixing [21]. As was recently pointed out by several groups [22, 23], most of these studies make the assumption that the response of the metal is linear and that the nonlinearity only originates from the dielectric medium adjacent to the metal. De Leon *et al.* [22] and Marini *et al.* [23] argue that past experimental work has shown that the third-order nonlinear susceptibility $\chi^{(3)}$ of metals can be enormous and can exhibit ultrafast behavior at optical wavelengths; this opens up the possibility of designing nonlinear plasmonic devices based on the intrinsic nonlinear response of the metallic component of the structure.

There is a great deal of uncertainty regarding the value of $\chi^{(3)}$ for metals - notably for gold, for instance - due to the strong frequency dispersion of metal nonlinear susceptibilities at wavelengths below 800 nm. Past measurements of $\chi^{(3)}$ have exhibited a variation in magnitude of more than four orders of magnitude, with a strong dependence on pulse duration [24]. In spite of this, it is important to determine the scaling of the nonlinear response from both the metal and the dielectric for a range of experimental conditions such as laser wavelength, pulse duration, metal/dielectric combination and geometry. For this reason, we introduce here an analytical figure-of-merit to assess the dominant nonlinear response of a nonlinear plasmonic system. We apply this metric to the simplest case of a plasmonic waveguide: a single metal/dielectric interface and focus on the case of gold to determine whether the dielectric or the gold nonlinear response dominates for several dielectrics. We study self-action of the SPP through the third-order nonlinearity and use full-wave numerical simulations to determine which nonlinear responses dominate in an optical switching scenario.

Structure investigated and analytical derivation of the figure of merit.

In the following, we consider solely a metal/dielectric interface as sketched in Fig. 1a. It consists of a semi-infinite metal slab that occupies the region $y < 0$ that is adjacent to a dielectric that occupies the region $y > 0$. The transverse profiles of the y- and x-component of the electric field are sketched on the figure. The spatial dependence of the surface plasmon polariton (SPP)

field propagating in the positive x direction is given by $\psi_{\mathrm{SPP}}(x,y)=\left[H_z(x,y),E_x(\mathrm{x},\mathrm{y}),E_y(x,y)\right]$ and may be written in the form [25]

$$\psi_{\mathrm{SPP}}(x,y)=E_0\exp\left(ik_0n_{\mathrm{SPP}}x\right)\begin{cases}\exp\left(ik_0n_\perp^{\mathrm{d}}y\right)\left[1/\mathrm{Z}_0,-\dfrac{n_\perp^{\mathrm{d}}}{\varepsilon_{\mathrm{d}}},\dfrac{n_{\mathrm{SPP}}}{\varepsilon_{\mathrm{d}}}\right], & \text{for } y>0\\ \exp\left(-ik_0n_\perp^{\mathrm{m}}y\right)\left[1/\mathrm{Z}_0,\dfrac{n_\perp^{\mathrm{m}}}{\varepsilon_{\mathrm{m}}},\dfrac{n_{\mathrm{SPP}}}{\varepsilon_{\mathrm{m}}}\right], & \text{for } y<0\end{cases}, \qquad (1)$$

where $k_0 = 2\pi/\lambda_0$, $n_{\mathrm{SPP}}=\sqrt{\varepsilon_{\mathrm{d}}\varepsilon_{\mathrm{m}}/(\varepsilon_{\mathrm{d}}+\varepsilon_{\mathrm{m}})}$ is the effective index of the SPP mode, $n_\perp^{\mathrm{d}}=\sqrt{\varepsilon_{\mathrm{d}}-n_{\mathrm{SPP}}^2}$, $n_\perp^{\mathrm{m}}=\sqrt{\varepsilon_{\mathrm{m}}-n_{\mathrm{SPP}}^2}$, Z_0 is the impedance of free-space, ε_{m} is the dielectric constant of the metal, and ε_{d} is that of the dielectric. From Eq. (1), we see that the ratio of the y-component to the x-component of the electric field in the dielectric (metal) is equal to $\left|n_{\mathrm{SPP}}/n_\perp^{\mathrm{d}}\right|$ ($\left|n_{\mathrm{SPP}}/n_\perp^{\mathrm{m}}\right|$). Because we are mostly interested in third-order nonlinear processes in isotropic materials in which the polarization mostly couples back to the SPP field (self-action), we find it useful to consider the ratio $\left|E_y/E_x\right|^4$ in the metal and dielectric regions, to determine the dominant field orientations and simplify the analytical expression for the figure-of-merit. Before focusing on the specific case of the gold interface with an arbitrary dielectric, we consider first the field component ratio for several metal interfaces having a common dielectric. For the spectral variations of ε_{m}, we use the data from Palik's handbook for both gold and silver [26] and from Rakic *et al*. [27] for aluminium and copper and obtain the results in Fig. 1b, which compares the wavelength dependence of this ratio for $\varepsilon_{\mathrm{d}} = 5$ – a value that is typical for chalcogenide glasses.

For all metals, the field component ratio is large in the dielectric and small in the gold for wavelengths toward the red-end of the visible spectrum (*i.e.*, above 600 nm), such that we may make the approximation that the total nonlinear polarization in the dielectric is mostly driven by the y-component of the electric field, whereas the total nonlinear polarization in the metal is mostly driven by the x-component of the electric field. This approximation is even more valid in the infrared, where the characteristic Drude model response of the metal is dominant, such that $\left|E_y/E_x\right|$ scales more or less as $\sqrt{\varepsilon_{\mathrm{Au}}/\varepsilon_{\mathrm{d}}}$ in the dielectric and is vanishingly small in the metal region. It is interesting that this approximation is not valid at wavelengths below 600 nm where

the interband transitions of metals dominate for gold, silver and copper. On the other hand, aluminium, whose interband transition lies in the deep ultraviolet, displays identical behavior for all wavelengths above 300 nm.

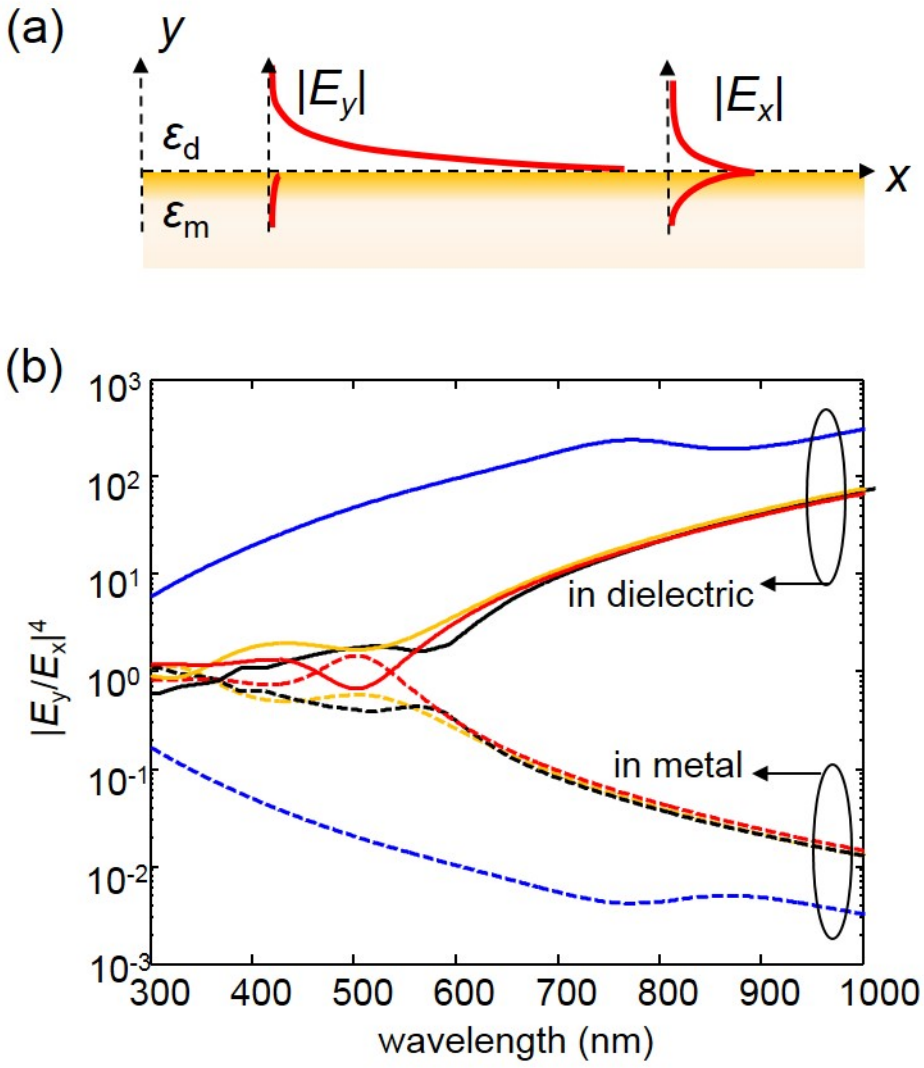

Fig. 1. **Structure investigated and scaling of the electric field components.** (a) Illustration of the single gold-dielectric interface. The transverse profiles of the modulus of both the *y*- and *x*-components of the field associated with the SPP mode are shown. (b) Spectral dependence of $|E_y/E_x|^4$ in the dielectric (solid lines) and in the metal (dashed lines) for $\varepsilon_d = 5$ and for different metals (black : silver, red : gold, orange : copper and blue : aluminium).

Under these approximations and for the case of self-action, the third-order nonlinear polarization may be decoupled for each half-space as

$$P_{\mathrm{d}}^{(3)}(x,y) = \frac{3}{4}\varepsilon_0 \chi_{\mathrm{d}}^{(3)} \left| E_y^{\mathrm{d}}(x,y) \right|^2 E_y^{\mathrm{d}}(x,y)\,, \tag{2}$$

$$P_{\mathrm{m}}^{(3)}(x,y)=\frac{3}{4}\varepsilon_0\chi_{\mathrm{m}}^{(3)}\left|E_x^{\mathrm{m}}(x,y)\right|^2 E_x^{\mathrm{m}}(x,y), \tag{3}$$

where the *d* and *m* subscripts and superscripts refer to the dielectric and metal, respectively, $P^{(3)}$ is the third-order nonlinear polarization, and $\chi^{(3)}$ is the third-order nonlinear susceptibility. The relative importance of the dielectric nonlinear response in comparison to the metal nonlinear response is quantified by the ratio ρ of the spatial overlap integral in each medium between the nonlinear polarization and the SPP mode profile

$$\rho=\left|\frac{\int P_{\mathrm{d}}^{(3)}(x,y)E_{\mathrm{d}}^{*}(x,y)dy}{\int P_{\mathrm{m}}^{(3)}(x,y)E_{\mathrm{m}}^{*}(x,y)dy}\right|. \tag{4}$$

This ratio is derived by treating the nonlinearity as a perturbation and considering its effect on the propagating SPP mode through coupled-mode theory [28, 29]. A justification for considering this ratio is derived in the Appendix. Here, we only consider unidirectional propagation of the SPP mode and neglect any back-scattering of the forward propagating mode and the nonlinear response. By introducing Eqs. (2) and (3) into Eq. (4) and making the approximation that $E_{\mathrm{d}} \sim E_y^{\mathrm{d}}$ and $E_{\mathrm{m}} \sim E_x^{\mathrm{m}}$ every time a fourth power of the modulus is involved, we obtain a convenient closed form expression for ρ given by

$$\rho=\left|\frac{\chi_{\mathrm{d}}^{(3)}}{\chi_{\mathrm{m}}^{(3)}}\right|\left|\frac{\mathrm{Im}\left(n_{\perp}^{\mathrm{m}}\right)}{\mathrm{Im}\left(n_{\perp}^{\mathrm{d}}\right)}\right|\left|\frac{n_{\mathrm{SPP}}}{\varepsilon_{\mathrm{d}}}\right|^4\left|\frac{\varepsilon_{\mathrm{m}}}{n_{\perp}^{\mathrm{m}}}\right|^4 \tag{5}$$

This ratio is used below to determine which of the two nonlinear responses dominates and it only depends on the material linear and nonlinear parameters.

Scaling of the nonlinear response for different gold/dielectric combinations.

From Eq. (5), we see that ρ depends most importantly on the ratio of $\left|\chi_{\mathrm{m}}^{(3)}/\chi_{\mathrm{d}}^{(3)}\right|$ and on ε_{d}. We now focus on the case of a gold/dielectric interface. Figure 2 is a contour plot showing the scaling of ρ with these two quantities for an interface involving gold. The solid black curve represents the limiting case where $\rho = 1$, above which the gold nonlinear response is dominant and below which the dielectric nonlinear response is dominant. This graph is convenient as it enables us to identify the relevant nonlinear response for any gold/dielectric combination, solely based on the knowledge of $\chi^{(3)}$ and ε_{d}. The values used to compute Fig. 2 are given in Table 1.

Of course, knowing the $\chi^{(3)}$ of gold is paramount to computing this graph and its value should be chosen carefully from the wide range of published values. Indeed, there is a strong dispersion of experimentally measured values of $\chi^{(3)}$, both with wavelength and with the pulse durations used to make the measurement, which is due to the many processes contributing to the third-order nonlinear response in gold [24]. Very recently De Leon *et al.* [30] measured a value of $\chi^{(3)} = (4.67+i3.03)\times10^{-19}$ (m^2/V^2) using the Kretschmann-Raether configuration at $\lambda = 800$ nm. Their setup is remarkably sensitive to the nonlinear response of a thin gold film. The experiment was carried out with very short laser pulses (~ 100 fs) for which the relevant nonlinearity is believed to be the smearing of the Fermi-Dirac distribution function due to hot electrons [31]. As the pulse duration is increased, the third-order nonlinearity gradually transfers to a thermal nonlinearity with the heating of the lattice due to the hot electron relaxation, yielding values which are typically 100 times larger than the ultrafast value and which are often used to make theoretical predictions [22,23].

Material	ε_d	$\chi_d^{(3)}$ (m^2/V^2) $\times 10^{19}$	$\left\|\chi_{Au}^{(3)} / \chi_d^{(3)}\right\|$	λ (μm)	Ref.
Al_2O_3	3.24	0.0031	1800	1.06	[32]
GaAs	12	24+*i*48	0.2	1.55	[33]
Si	11.6	25+*i*0.0039	0.2	1.55	[34]
TiO_2	6.15	0.21	27	1.06	[32]
SiO_2	2.25	0.0025	2200	1.3	[32]
As_2Se_3	5.76	4.1+*i*0.56	1.4	1.5	[35]
Bi_2O_3	6.25	0.24	23	1.5	[35]
4BCMU	2.43	-1.3+*i*0.55	4.3	1.06	[32]
Air	1.000 6	1.7×10^{-6}	3×10^{6}		[32]

Table 2. **Linear and nonlinear parameters of the dielectrics considered in our simulations.** Values have been gathered either from direct values of $\chi^{(3)}$ or from values of the intensity dependent refractive index $n_2 = 3\mathrm{Re}[\chi^{(3)}]/(4n_0^2\varepsilon_0 c)$ (when n_2 has units of m^2/W) and the nonlinear absorption coefficient $\beta = 3\omega\mathrm{Im}[\chi^{(3)}]/(2n_0^2\varepsilon_0 c^2)$, when relevant. The value used here for the $\chi^{(3)}$ of gold is $(4.67+i3.03)\times10^{-19}$ (m^2/V^2) and is taken from De Leon *et al.* [30].

To produce Table 1 and compute ρ, we used the value measured by De Leon *et al.* [30]. Figure 2 shows that the nonlinear response of gold dominates for the case of weakly nonlinear dielectrics such as silicon dioxide and aluminium oxide. However, for strongly nonlinear

dielectrics such as highly nonlinear polymers like polydiacetylenes (4BCMU) or chalcogenide glasses (As_2Se_3) or even semiconductors (GaAs and Si), it is the dielectric nonlinear response that is dominant. Some cases are more difficult to determine, such as with titanium oxide, or with bismuth oxide and are likely to involve competition between the nonlinearities in each domain. It should be noted that the graph was produced for $\lambda = 800$ nm, but certainly captures the essential physics for wavelengths in the near infrared since $\chi^{(3)}$ of gold is mostly constant for wavelengths greater than 750 nm [23] and since the SPP mode profile remains almost identical because of weak dispersion for most of the dielectrics considered here. For shorter wavelengths, obviously, the graph will be greatly modified due to the strong wavelength dispersion of both $\chi^{(3)}$ of gold and the SPP.

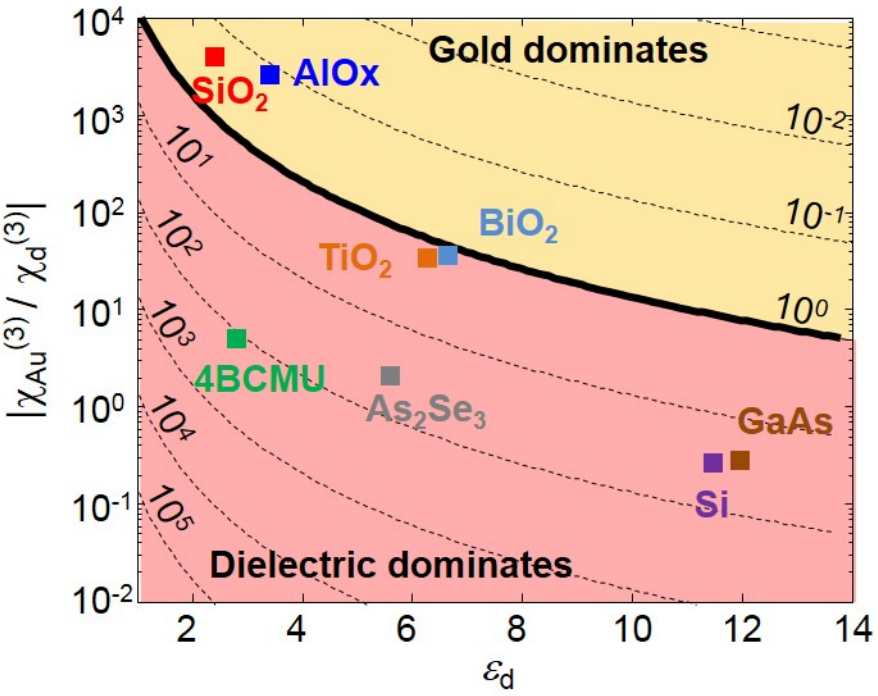

Fig. 2. **Mapping of the nonlinear response for a gold/dielectric interface.** Contour plot of ρ, given by Eq. (5) as a function of the modulus of the ratio of the third-order nonlinear susceptibilities of gold and the dielectric material and of the real part of ε_d. The black continuous curve denotes the $\rho = 1$ limiting case above which the gold nonlinear response is stronger and below which the dielectric response is stronger. Several nonlinear dielectrics are indicated on the graph.

Full-wave simulations: the case of optical switching of the SPP.

Next, we use full-wave numerical simulations using the commercial software COMSOL Multiphysics based on the finite-element method and verify that the behavior shown in Fig. 2 can be used to understand optical switching of the SPP for a subset of dielectrics.

Optical switching of the SPP is a self-induced process in which the third-order nonlinear polarization given by Eqs. (2) and (3) produces an intensity-dependent modulation of the dielectric constant, given by

$$\varepsilon = \varepsilon_{\mathrm{L}} + \frac{3}{4}\chi^{(3)}|E|^2 , \tag{6}$$

where ε_{L} is the linear dielectric constant. This modulation in turn produces a modulation of the SPP effective mode index n_{SPP}, which causes a decrease in the SPP propagation length, defined as the $1/e$ decay length of the SPP intensity. In the linear case, it is simply equal to

$$l_{\mathrm{SPP}} = \frac{\lambda}{4\pi\,\mathrm{Im}[n_{\mathrm{SPP}}]} . \tag{7}$$

In some cases, the modulation of n_{SPP} can produce an increase of l_{SPP}. The relative increase or decrease in l_{SPP} depends on the signs of both the real and imaginary parts of $\chi^{(3)}$. For instance, we expect an increase of l_{SPP} at λ = 500 nm, where both real and imaginary parts of $\chi^{(3)}$ of gold are negative.

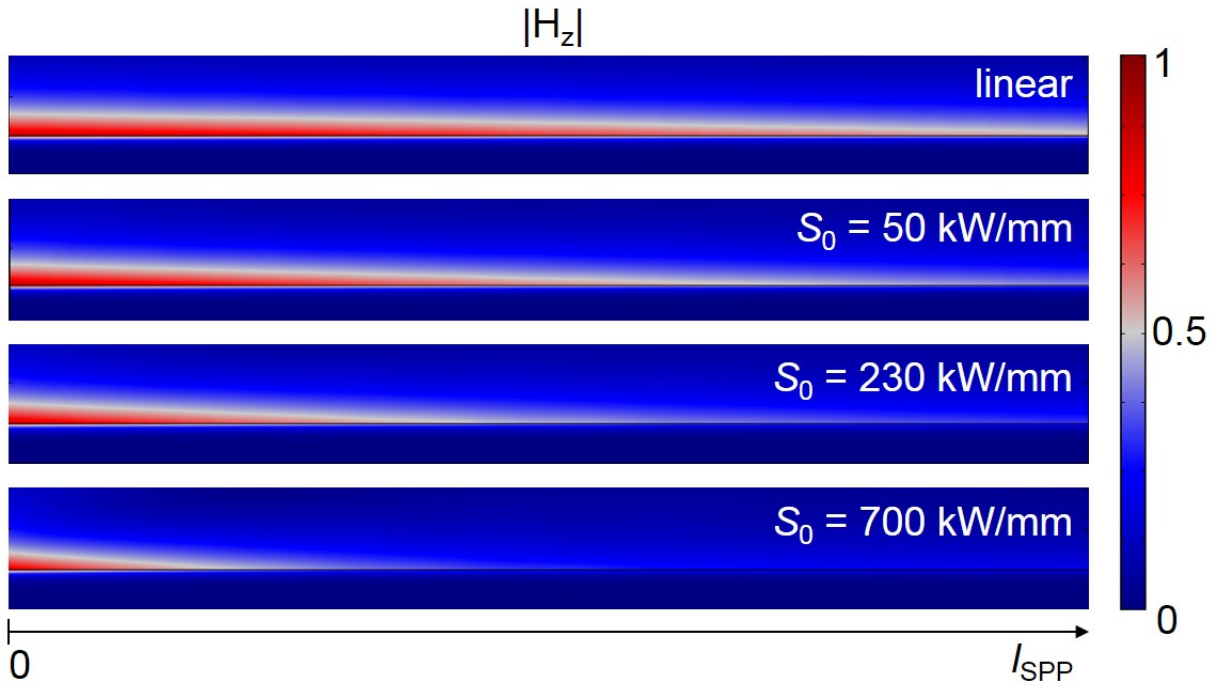

Fig. 3. **Nonlinear propagation of the SPP field.** Modulus of the magnetic field H_z calculated for a gold/GaAs interface at λ = 1.5 μm over a length equal to the propagation length of the surface plasmon in the linear regime for different values of S_0. The linear and nonlinear properties of the GaAs are given in Table 1. Each plot is normalized to the input value of $|H_z|$.

The total electromagnetic field of the single interface problem is computed in a 2D configuration when excited by the SPP mode for a fixed waveguide length. Both the semi-infinite half-planes (gold and dielectric) are defined with a diagonal dielectric constant tensor

$$\varepsilon = \varepsilon_{\mathrm{L}} I_3 + \frac{3}{4}\chi^{(3)} \begin{bmatrix} |E_x|^2 & 0 & 0 \\ 0 & |E_y|^2 & 0 \\ 0 & 0 & 0 \end{bmatrix}, \tag{8}$$

where I_3 is the 3×3 identity matrix and where the relevant values of ε_{L} and $\chi^{(3)}$ are introduced in each medium. The calculations are carried out as the input power per unit length S_0 carried by the SPP is varied. The power per unit length $S(x)$ along the z direction is defined as the power flow along the x direction of the time-averaged Poynting vector $S(x) = 1/2\,\mathrm{Re}\int_{-\infty}^{+\infty} \left(\mathbf{E}\times\mathbf{H}^*\right).\mathbf{e}_x dy$. Figure 3 shows the field distribution in the case of a gold/GaAs interface for different values of S_0 over a length equal to the SPP propagation length in the linear case. As expected, we observe that the field extends over smaller and smaller portions of the waveguide as S_0 is increased. This is due to the self-induced modulation of the effective mode index.

Next, we numerically calculate the propagation length of the SPP for several gold/dielectric combinations to determine its dependence with S_0 (see Fig. 4). For every combination, S_0 is varied to quantify the transition from the linear to the nonlinear regime, calculations are made by considering the nonlinear response of gold only (crosses), and of both the gold and the dielectric (circles). On the one hand, the threshold values of S_0, where the switching behavior occurs, are lower by about two orders-of-magnitude for the cases of GaAs and 4BCMU when the dielectric nonlinear response is included, clearly demonstrating that the nonlinearity of the dielectric dominates. The cases of air and silica, on the other hand, are very different as there is no noticeable difference in the optical switching of the SPP, whether the nonlinearity of the dielectric is included or not, which shows that the gold nonlinear response dominates. Both these observations are expected from the mapping of ρ (see Fig. 2).

The representation provided in Fig. 4 is quite convenient as it can be used to determine the potential size of a SPP switching device and the minimal control power required for operation. Bearing this in mind, we can provide a discussion on the values of S_0 in these simulations. First, it should be noted that the switching thresholds of S_0 scale proportionally with the inverse of $\chi^{(3)}$. This is indicated by the dotted curve in Fig. 4, which corresponds to a simulation of the gold/air interface when the $\chi^{(3)}$ of gold is equal to that found in [22,23], which is about two orders of magnitude larger than the $\chi^{(3)}$ used for the rest of the simulations. The variation of the propagation length in this case occurs at values of S_0 that are within an order-of-magnitude of those predicted by the De Leon *et al.* model [22], which investigates small variations of the propagation length (~10%). Second, the dashed line in Fig. 4 indicates the damage threshold of gold for pulses on the order of 100 fs [36], which shows that, in this specific situation studied here, the single gold/air and gold/SiO_2 interfaces would actually constitute poor optical switches given the $\chi^{(3)}$ for gold used in our present calculations. Higher $\chi^{(3)}$ values will reduce the switching threshold. Some dielectrics (4BCMU and GaAs) enable operation well below the optical damage threshold. We stress that our simulations represent a best case scenario in that we do not consider competing nonlinearities that are likely to appear when S_0 becomes large, such as free-carrier nonlinearities in GaAs or Si [33,34]. However the metric we have introduced and the analysis we provide can be applied to other situations, involving other nonlinear processes and different waveguide geometries to guide : a) the choice of the dielectric adjacent to gold, b) the device length and c) the command power required to operate a plasmonic device for a specific nonlinear application.

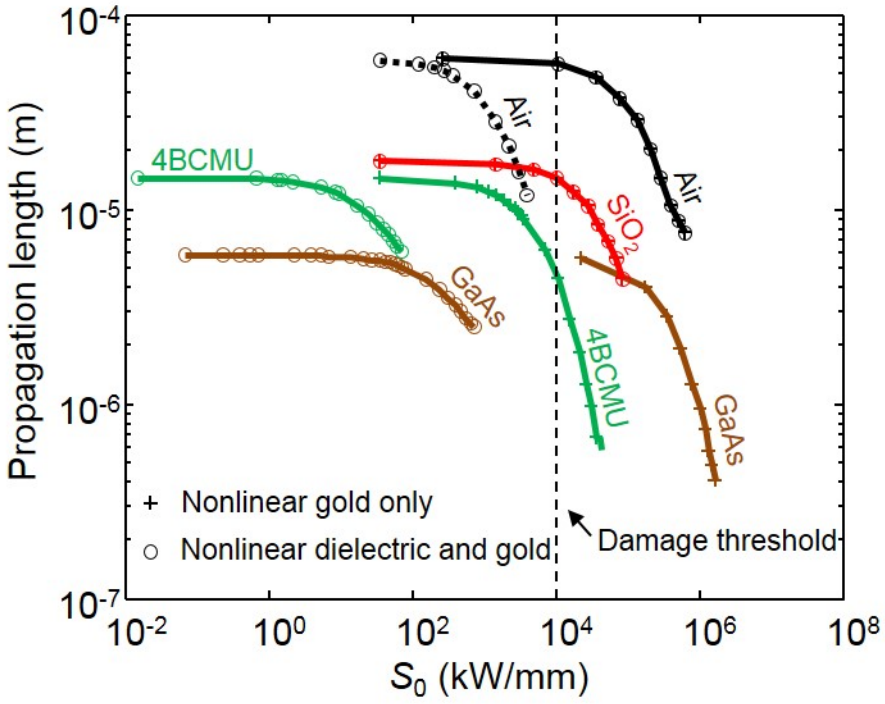

Fig. 4. **Optical switching of the SPP for different gold/dielectric combinations.** Propagation length of the SPP as a function of the input power per unit length S_0 for different dielectrics (black : air, red : SiO_2, green : 4BCMU and brown : GaAs). Crosses correspond to calculations that are carried out when only the gold nonlinear response is taken into account. Rings correspond to calculations that are carried out when both the gold and the dielectric nonlinear response are taken into account. The dotted curve is computed for the gold/air interface with the value of $\chi^{(3)}$ taken from Marini *et al.* [19]. The dashed line indicates the optical damage threshold of gold for 100 fs pulses.

In summary, we introduce a figure-of-merit ρ, which enables us to predict the dominant nonlinear response (metal or dielectric) for a given plasmonic problem. We evaluate this metric for the case of a single gold/dielectric interface for several nonlinear dielectrics and investigate configurations where the gold nonlinear response dominates and others where the dielectric nonlinear response dominates. Finally, we focus on self-action of the SPP through the third-order nonlinearity and verify which of the nonlinear responses dominates in the case of optical switching. Additional work is required to capture the essential physics that govern the complex nonlinear response of simple plasmonic architectures. The metric we have introduced can be applied to finite thickness metallic slabs surrounded by dielectrics or to finite thickness dielectric slabs surrounded by metals. Both structures present symmetric and anti-symmetric modes which are likely to present very different nonlinear behaviors that depend on the slab thickness, because

the transverse profiles of the electric field components are drastically different. In such cases however, ρ cannot be determined analytically because the dispersion relations of these waveguides do not have an analytical solution.

Acknowledgements

A. B. would like to thank Chistos Argyropoulos and Britt Lassiter for useful discussions on plasmonics and Patrick Bowen for discussions on coupled mode theory.

Appendix: Derivation of ρ

The single metal/dielectric interface is a single-mode waveguide for which the SPP field $\mathbf{E}_{\mathrm{SPP}}$ is a solution of the propagation equation

$$\left(\nabla^2 - \beta_{\mathrm{SPP}}^2\right)\mathbf{E} = 0\,, \tag{9}$$

where $\beta_{\mathrm{SPP}} = k_0 n_{\mathrm{SPP}}$ is the SPP propagation constant. Considering the third-order nonlinear polarization presented in Eqs. 2 and 3 to be a small perturbation, the nonlinear propagation equation of the perturbed case is given by

$$\left(\nabla^2 - \beta_{\mathrm{SPP}}^2\right)\mathbf{E} = \mu_0\omega^2\mathbf{P}^{(3)}\ . \tag{10}$$

From perturbation theory, we may consider $\alpha\mathbf{E}_{\mathrm{SPP}}$ to be a solution to Eq. (10), with $|\,\alpha\,| \sim 1$ and $arg(\alpha)\sim 0$. Then, by making the slowly varying envelope approximation ($\left\|\mathbf{E}_{\mathrm{SPP}}\nabla^2\alpha\right\| \ll \left\|2\nabla\alpha\nabla\mathbf{E}_{\mathrm{SPP}}\right\|$) and using Eq. (9), Eq. (10) reduces to

$$\mathbf{E}_{\mathrm{SPP}}\nabla\alpha = -\frac{i\mu_0\omega^2}{2\beta_{\mathrm{SPP}}}\mathbf{P}^{(3)}\ . \tag{11}$$

Applying the dot product with the complex conjugate of $\mathbf{E}_{\mathrm{SPP}}$ to both sides of Eq. (11) and integrating over the entire volume Ω of space, we obtain the relation

$$\nabla\alpha = -\frac{i\mu_0\omega^2}{2\beta_{\mathrm{SPP}}\Omega_{\mathrm{SPP}}}\left(\int_{\Omega_{\mathrm{m}}}\mathbf{P}^{(3)}\mathbf{E}_{\mathrm{SPP}}^{*}d\Omega + \int_{\Omega_{\mathrm{d}}}\mathbf{P}^{(3)}\mathbf{E}_{\mathrm{SPP}}^{*}d\Omega\right)\,, \tag{12}$$

where Ω_{m} and Ω_{d} represent the metal and dielectric half-volumes, respectively, and $\Omega_{\mathrm{SPP}} = \int_{\Omega}\left|E_{\mathrm{SPP}}\right|^2 d\Omega$ is the SPP mode volume. Factoring out the integral over the dielectric half-volume in the previous equation yields

$$\nabla\alpha = -\frac{i\mu_0\omega^2}{2\beta_{SPP}\Omega_{SPP}}\int_{\Omega_m}\mathbf{P}^{(3)}\mathbf{E}^*_{SPP}d\Omega\left(1+\frac{\int_{\Omega_d}\mathbf{P}^{(3)}\mathbf{E}^*_{SPP}d\Omega}{\int_{\Omega_m}\mathbf{P}^{(3)}\mathbf{E}^*_{SPP}d\Omega}\right). \quad (13)$$

We define the real quantity ρ as the magnitude of the ratio in Eq. (13)

$$\rho = \left|\frac{\int_{\Omega_d}\mathbf{P}^{(3)}\mathbf{E}^*_{SPP}d\Omega}{\int_{\Omega_m}\mathbf{P}^{(3)}\mathbf{E}^*_{SPP}d\Omega}\right|. \quad (14)$$

It is clear that $\rho << 1$ ($\rho >> 1$), implies that the nonlinear response is dominated by the metal (dielectric) half-volume. Because the single metal/dielectric interface is a one-dimensional problem, the volume integrals in Eq. (14) reduce to line integrals along a line orthogonal to the propagation direction, which yields Eq. (4). The calculation made here implicitly assumes that the nonlinear polarization included in Eq. (10) shares the same frequency as the electric field of the SPP mode.

It should be noted that, in the general case of subwavelength waveguides, such as microstructured fibers, a full vectorial model of nonlinear propagation is required to account for the role of the longitudinal component of the electric field, which can result in a totally different nonlinear behavior to that expected from classical nonlinear models [37]. The reason for this is that the fundamental mode can have two polarizations, which are not orthogonal to one another in the classical sense (*i.e.* for the transverse fields), if the longitudinal component of the electric field is strong. In such cases, the nonlinear propagation equation takes a different form to that presented in Eq. (12). We refer readers to Afshar *et al.* [37] for further reading on the subject, but this observation does not apply to plasmonic waveguides, because the fundamental mode only has a single polarization that is transverse magnetic.

References

1. G. Cerullo and S. De Silvestri, Rev. Sci. Instrum. **74**, 1 (2003).
2. M. Fejer, Phys. Today **47**, 25 (1994).
3. Y. Wang, C.-Y. Lin, A. Nikolaenko, V. Raghunathan, and E. O. Potma, Adv. Opt. Photon. **3**, 1 (2011).
4. D. Cotter, R. Manning, K. Blow, A. Ellis, and A. Kelly, Science **286**, 1523 (1999).

5. H. Raether, *Surface Plasmons on Smooth and Rough Surfaces and on Gratings* (Springer, 1998).

6. J. A. Schuller, E. S. Barnard, W. Cai, Y. C. Jun, J. S. White, and M. L. Brongersma, Nat. Materials **9**, 193 (2010).

7. J. Renger, R. Quidant, N. van Hulst, and L. Novotny, Phys. Rev. Lett. **104**, 059903 (2010).

8. A. Bouhelier, M. Beversluis, A. Hartschuh, and L. Novotny, Phy. Rev. Lett. **90**, 013903 (2003)

9. N. I. Zheludev, Science **328**, 582 (2010).

10. D. Mihalache, G. I. Stegeman, C. T. Seaton, E. M. Wright, R. Zanoni, A. D. Boardman, and T. Twardowski, Opt. Lett. **12**, 187 (1987).

11. H. Yin, C. Xu, and P. M Hui, Appl. Phys. Lett. **94**, 221102 (2009).

12. J.-H. Huang, R. Chang, P.-T. Leung, and D. P. Tsai, Opt. Commun. **282**, 1412 (2009).

13. A. R. Davoyan, I. V. Shadrivov, and Y. S. Kivshar, Opt. Express **16**, 21209 (2008).

14. A. Degiron, and D. R. Smith, Phys. Rev. A **82**, 033812 (2010).

15. Y. Liu, G. Bartal, D. A. Genov, and X. Zhang, Phys. Rev Lett. **99**, 153901 (2007).

16. E. Feigenbaum, and M. Orenstein, Opt. Lett. **32**, 674 (2007).

17. K. F. MacDonald, Z. L. Samson, M. I. Stockman, and N. I. Zheludev, Nat. Photon. **3**, 55 (2009).

18. A. R. Davoyan, I. V. Shadrivov, A. A. Zharov, D. K. Gramotnev, and Y. S. Kivshar, Phys. Rev. Lett. **15**, 116804 (2012).

19. R. E. Noskov, P. A. Belov, and Y. S. Kivshar, Phys. Rev. Lett. **108**, 093901 (2012).

20. R. E. Noskov, A. E. Krasnok, and Y. S. Kivshar, New J. Phys. **14**, 093005 (2012).

21. H. Suchowski, K. O'Brien, Z. J. Wong, A. Salandrino, X. Yin, and X. Zhang, Science **342**, 1223 (2013).

22. I. De Leon, J. E. Sipe, and R. W. Boyd, Phys. Rev. A **89**, 013855 (2014).

23. A. Marini, M. Conforti, G. Della Valle, H. W. Lee, Tr. X. Tran, W. Chang, M. A. Scmidht, S. Longhi, P. St. J. Russell, and F. Biancalana, New J. Phys. **15**, 013033 (2013).

24. R. W. Boyd, Z. Shi, and I. De Leon, Opt. Commun. **326**, 74 (2014).

25. P. Lalanne, J. P. Hugonin, H. T. Liu, and B. Wang, Surf. Sci. Rep. **64**, 453 (2009).

26. E. D. Palik, *Handbook of Optical Constants of Solids* (Academic Press, New York, 1985).

27. A. D. Rakic, A. B. Djurisic, J. M. Elazar, and M. L. Majewski, Appl. Opt. **37**, 5271 (1998).

28. A. Yariv, IEEE J. of Quantum Electron. **9**, 919 (1973).

29. G. P. Agrawal, *Nonlinear Fiber Optics*, 4th ed, Ch. 2 (Academic Press, 2007)

30. I. De Leon, Z. Shi, A. C. Liapis, and R. W. Boyd, Opt. Lett. **39**, 15 (2014).

31. F. Hache, D. Ricard, C. Flytzanis, and U. Kreibig, Appl. Phys. A **47**, 347 (1988).

32. R. W. Boyd, *Nonlinear Optics*, 3rd ed, Ch. 4 (Academic Press, New York, 2008).

33. A. Baron, A. Ryasnyanskiy, N. Durbreuil, P. Delaye, Q. V. Tran, S. Combrié, A. de Rossi, R. Frey, and G. Roosen, Opt. Express **17**, 552 (2009).

34. A. Baron, N. Dubreuil, P. Delaye, R. Frey, and G. P. Agrawal, J. Eur. Opt. Soc. **6**, 11030 (2011).

35. B. J. Eggleton, B. Luther-Davies, and K. Richardson, Nat. Photon. **5**, 141 (2011).

36. J. Krüger, D. Dufft, R. Koter, and A. Hertwig, Appl. Surf. Science **253**, 7815 (2007).

37. S. Afshar V., and T. M. Monro, Opt. Express **17**, 2298 (2009).